Patterns of Oligodendrocyte Pathology in Coronavirus-Induced Subacute Demyelinating Encephalomyelitis in the Lewis Rat

VESNA BARAC-LATAS,[1] GERDA SUCHANEK,[2] HELENE BREITSCHOPF,[3] ALBERT STUEHLER,[4] HELMUT WEGE,[5] AND HANS LASSMANN[3]*
[1]*Department of Physiology and Immunology, University of Rijeka, C-51000 Rijeka, Croatia*
[2]*Austrian Academy of Sciences, A-1010 Vienna, Austria*
[3]*Clinical Institute of Neurology, University of Vienna, A-1090 Vienna, Austria*
[4]*Institute of Virology and Immunology, University of Wuerzburg, D-97078 Wuerzburg, Germany*
[5]*Institute of Diagnostic Virology, Federal Research Center for Virus Diseases of Animals, Friedrich-Loeffler-Institutes, D-17498 Insel Riems, Germany*

ABSTRACT   Intracerebral infection of rats with JHM coronavirus induces a chronic inflammatory demyelinating disease, which in many respects mimicks the pathology of multiple sclerosis. We investigated the patterns of demyelination and oligodendrocyte pathology in this model. In early stages of the disease infection of oligodendrocytes was associated with a downregulation of expression of mRNA for proteolipid protein in the absence of myelin destruction. When demyelinating lesions were formed infected oligodendrocytes were destroyed by necrosis, whereas oligodendrocytes that did not contain detectable virus antigen or RNA were in part dying by apoptosis. At this stage of the disease remyelination of the lesions was pronounced. At later stages after infection virus antigen was nearly completely cleared from the lesions. In spite of the lack of detectable virus, ongoing demyelination and unspecific tissue destruction occurred, and oligodendrocytes were mainly destroyed by apoptosis. These late lesions revealed only minimal central remyelination, but they were frequently repaired by Schwann cells. Our studies suggest that the mechanisms of myelin destruction in this model of virus-induced demyelination are complex and that the patterns of tissue damage may change during the course of the disease. *GLIA 19:1–7, 1997*   © 1997 Wiley-Liss, Inc.

INTRODUCTION

Coronavirus-induced subacute demyelinating encephalomyelitis (SDE) is a disease in rats that in several respects resembles human inflammatory demyelinating diseases, including multiple sclerosis (Kyuwa and Stohlman, 1990; Sorensen et al., 1980). After intracerebral infection it starts with an acute encephalomyelitis, characterized by virus infection of both neurons and glial cells and by severe inflammation and destructive lesions, located predominantly in the gray matter (Nagashima et al., 1978, 1979; Wege et al., 1984; Zimprich et al., 1991). When this stage is survived by the animals, a subacute demyelinating disease follows (Nagashima et al., 1978; Zimprich et al., 1991). In this stage virus infection is restricted to the glial cell population, equally affecting astrocytes and oligodendrocytes. Chronic persistent inflammation is associated with primary demyelination, some axonal pathology, and a variable degree of astrocyte destruction. In later stages, lesions may become remyelinated by both oligodendrocytes or Schwann cells.

A variety of different pathogenetic mechanisms have been suggested to be responsible for demyelination in

virus-induced encephalomyelitis. First, demyelination may be caused by direct virus-induced destruction of oligodendrocytes. This mechanism appears to be unlikely, since coronavirus infection in immunodeficient mice does not lead to demyelination (Fleming et al., 1993; Wang et al., 1990). On the other hand, demyelination may be mediated by the immune system, by a direct T-cell mediated cytotoxicity against virus-infected oligodendrocytes (Lindsley et al., 1991; Subak-Sharpe et al., 1993), by antibodies against viral envelope proteins that are expressed on the surface of oligodendrocytes (Zimprich et al., 1991), or just by toxic-macrophage products, liberated in the lesions (Botteron et al., 1992; Griot et al., 1989).

Although the primary nature of the demyelination in coronavirus-induced SDE is well documented, surprisingly little is known about the fate of oligodendrocyte in situ. From studies of this and other models there is good agreement that oligodendrocytes are infected by the virus and that infected oligodendrocytes show a decreased expression of RNA of their different myelin proteins (Jordan et al., 1989; Ozden et al., 1993; Rodriguez et al., 1994; Yamada et al., 1990). Although some oligodendrocytes appear to be lost from established lesions, little is known about the extent and patterns of oligodendrocyte destruction. In the present study we have approached this question by immunocytochemistry and in situ hybridization, using a pannel of antibodies and probes that are able to recognize oligodendrocytes at different stages of their differentiation and maturity (Breitschopf et al., 1992; Brueck et al., 1994; Ozawa et al., 1994). In addition, we have applied new techniques for the detection of dying cells through the visualization of nuclear DNA fragmentation (Gold et al., 1994; Iseki, 1986). Our results suggest a complex pattern of oligodendrocyte pathology that changes during different stages of the disease.

MATERIALS AND METHODS
Induction of Disease

The murine coronavirus strain MHV-JHM was passaged by intracerebral infection of mice and adapted to grow on Sac-cell cultures (Nagashima et al., 1978; Wege et al., 1984). Specific pathogen-free Lewis rats were obtained from the Zentralinstitut fuer Versuchstierzucht, Hannover (FRG). The rats were intracerebrally inoculated with 800 PFU of the MHV-JHM virus between 3 and 8 weeks of age.

Tissue Processing

Animals were ether anesthetized and perfused with 4% paraformaldehyde dissolved in 0.1 M phosphate buffer. Parts of the brain and spinal cord were routinely embedded in paraffin. Paraffin sections (3 μm thick) were stained with hematoxylin and eosin, Luxol fast blue for myelin, and Bielschowsky silver impregnation for axons.

Immunocytochemistry was performed with a biotin/avidin or alkaline phosphatase/anti-alkaline phosphatase technique as previously described in detail (Vass et al., 1986, 1989). The following primary antibodies and sera were used: a polyclonal rabbit anti-JHM serum (Wege et al., 1984); a polyclonal rabbit anti-proteolipid protein (PLP) serum (Gunn et al., 1990); monoclonal antibodies against glial fibrillary acidic protein (GFAP; Boehringer, Mannheim, FRG); myelin basic protein (MBP; Hybritec, USA); myelin oligodendrocyte glycoprotein (MOG; 8-18C5; a gift from Dr. C. Linington, Martinsried, FRG), 2′-3′-cyclic nucleotide 3′-phosphodiesterase (CNP; Affinity Research Products, Ilkeston, UK); macrophages (ED1; Serotec, UK); and T-lymphocytes (W3/13; Seralab, UK). For control, immune reactions were performed in the absence of primary antibodies or by using irrelevant antibodies of the same immunoglobulin class.

In Situ Hybridization

For in situ hybridization, dioxygenin-labeled riboprobes specific for PLP (Colman et al., 1982) and for coronavirus RNA (Winter, 1992) were used. The technique of in situ hybridization has been described in detail (Breitschopf et al., 1992). The specificity of the reaction was controlled by comparing hybridization with antisense and sense probes. Following in situ hybridization, the sections were either stained with hematoxylin or subjected to immunochemistry for PLP protein as described above.

In Situ Tailing

For detection of DNA fragmentation the technique described by Gold et al. (1994) was used. Briefly, deparaffinized sections were incubated for 1 h at 37°C with 50 μl of a reaction mixture containing 10 μl 5× tailing buffer, 1 μl digoxigenin DNA labeling mixture, 2 μl 25 mmol $CoCl_2$, 0.5 μl terminal transferase, and 36.5 μl distilled water. All reagents were obtained from Boehringer Mannheim (FRG). This was followed by three rinses in Tris-buffered saline and incubation with alkaline phosphatase-labeled anti-digoxigenin antibody (1:250). Alkaline phosphatase was visualized with fast red BB salt (Sigma) as a chromogen. After in situ tailing, the sections were either stained with hematoxylin or subjected to immunocytochemistry, using antibodies against T-cells, MOG, CNP, GFAP, or JHM virus. In addition, some sections were reacted with in situ tailing after in situ hybridization for PLP mRNA.

Quantitative Evaluation

Quantitative studies were performed on brain and spinal cord tissue of 19 rats in different stages of the
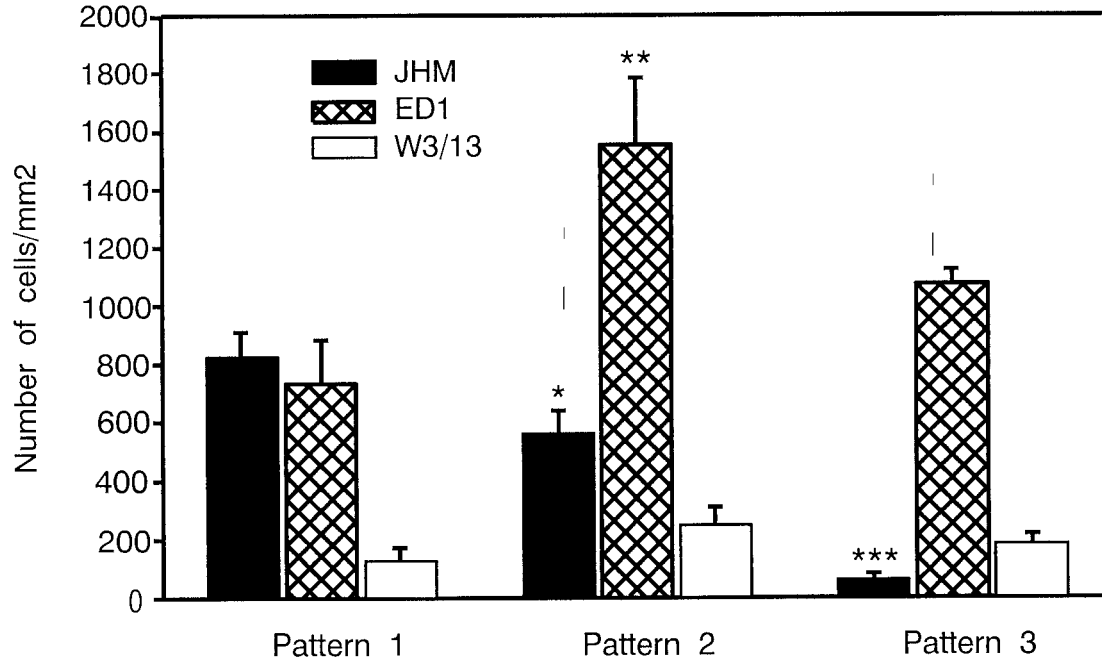
Fig. 1. Quantitative determination of JHM-virus antigen expressing cells and inflammatory cells in different lesional patterns. *, $P < 0.05$; **, $P < 0.01$; ***, $P < 0.001$ in comparison with pattern 1.

disease. Immunostained cells as well as cells positive in the in situ hybridization and in situ tailing reactions were counted in 10–25 high power fields, each covering an area of 0.01 mm^2. In addition, for detailed comparison of cell densities between lesions and control tissue, the exact areas covered by the lesions were matched topographically with sections of uninfected rats and identical counts performed in the respective control material. Values, given in Table 1 and in the figures are expressed as either cells/mm^2 or percentage of cell density in lesions compared with the matched control areas. A non-parametric group test (Mann-Whitney U test) was used to analyze statistical differences between the different disease stages.

RESULTS

The study was restricted to rats that had survived acute encephalomyelitis and had entered the demyelinating stage of the disease. Out of a larger sample of animals that were investigated in the course of other virological and immunological studies (Flory et al., 1995; Koerner et al., 1991; Wege et al., 1993; Zimprich et al., 1991), 19 rats were selected that contained widespread lesions at different phases of the demyelinating process 23–96 days after infection (Table 1). Clinically these animals presented with ruffled fur, an atactic, trembling gait and paralysis of hind legs that appeared 3–5 weeks after virus inoculation. According to pathological findings (Fig. 1) three patterns of the demyelinating disease were differentiated.

Pattern 1

This pattern was characterized by massive virus infection, mainly affecting the white matter of the spinal cord, the brain stem, and the cerebellar white matter. Forebrain lesions were sometimes encountered too, but they were rare. Virus-infected cells were identified as astrocytes and oligodendrocytes and were distributed in large plaques of infected cells, separated by uninfected normal central nervous system (CNS) tissue (Fig. 2d,f). The inflammatory reaction mainly consisted of lymphocytes and macrophages, located predominantly at the sites of infection (Figs. 1, 2c).

By conventional light microscopy, in these early lesions of the disease neither primary demyelination nor other tissue damage was observed (Fig. 2a), and immunoreactivity for different myelin proteins, such as MBP, PLP, MOG, and CNP, was similar, compared with that in the unaffected white matter; immunocytochemistry for GFAP showed increased reactivity of astrocytes.

Oligodendrocytes, identified by immunochemistry for CNP or MOG were larger in the infected areas, compared with the surrounding normal white matter. However, in situ hybridization revealed a downregulated expression of PLP mRNA, also evidenced by the significant numerical decrease of PLP mRNA-reactive oligodendrocytes in the lesions (Figs. 2b,e, 3). Staining with in situ hybridization for PLP mRNA and immunochemistry for virus protein in adjacent serial sections revealed that the decreased expression of mRNA was restricted to virus-infected areas (Fig. 2b,d).

BARAC-LATAS ET AL.

TABLE 1. Synopsis of animals with coronavirus-induced subacute demyelinating encephalomyelitis[a]

	No. of animals	Disease duration[1]	Time post virus inoculation[1]
Pattern I + II	9	3.3 ± 0.6 (1–6)	30.7 ± 1.9 (23–38)
Pattern III[b]	7	9.9 ± 2.2* (1–16)	47.1 ± 8.5* (26–96)

[a]Values are days, mean ± SEM, with range in parentheses.
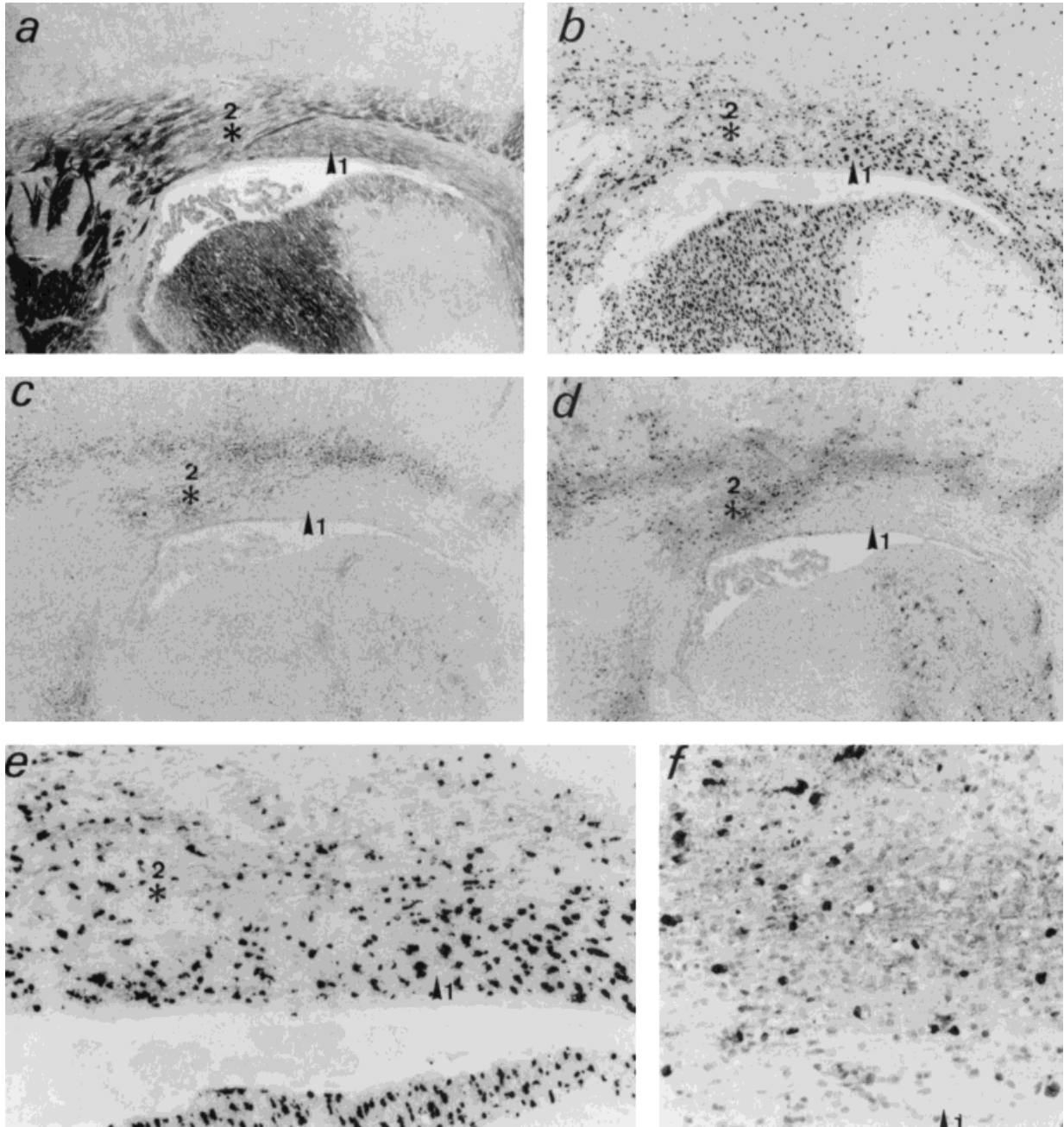[b]Pattern III is significantly different from pattern I and II.
*$P < 0.05$.

Fig. 2. Lesional pattern 1; serial sections through the periventricular white matter. **a:** Luxol fast blue. **b, e:** In situ hybridization for PLP mRNA. **c:** ED1-positive macrophages. **d, f:** JHM-virus antigen expression. Arrowhead 1 and asterisk 2 label identical positions on the different serial sections; areas with high virus antigen expression show reduced expression of PLP mRNA and some macrophage infiltration. **a–d,** ×50; **e,** ×150; **f,** ×200.
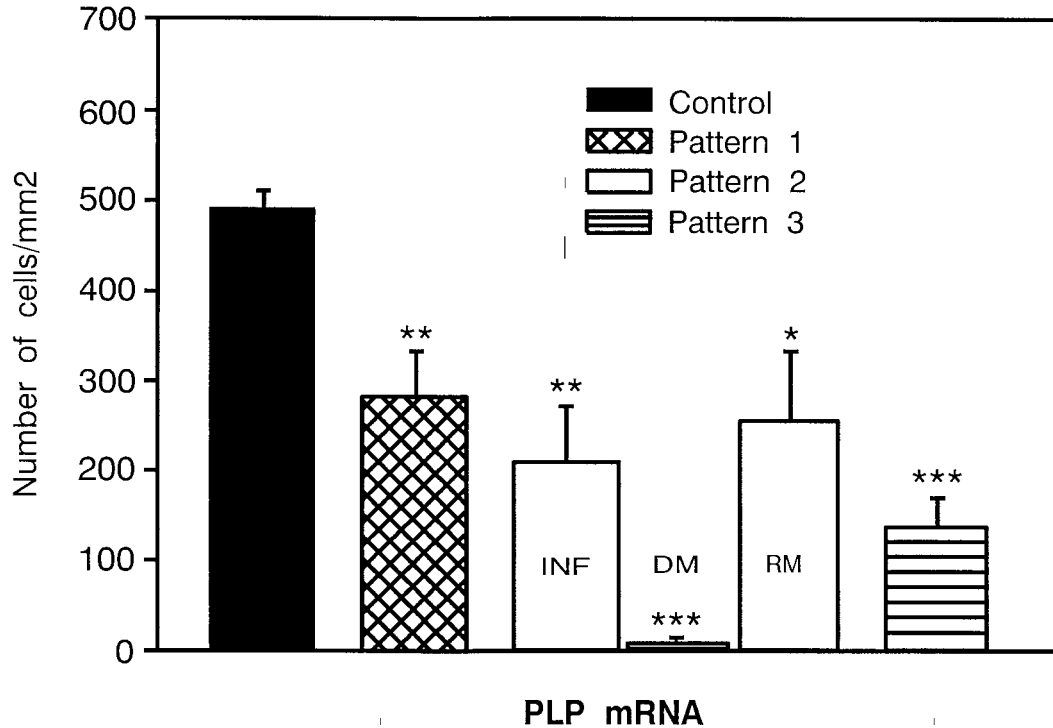
Fig. 3. Histogram showing downregulation of PLP mRNA expression in oligodendrocytes throughout the disease in Lewis rats with SDE in comparison with uninfected controls. For detailed comparison of cell densities between lesions and control tissue, the exact areas covered by the lesions were matched topographically with sections of uninfected rats. INF, virus-infected area surrounding the plaque; DM, demyelinated area; RM, remylinated area inside the plaque. $*$, $P < 0.05$; $**$, $P < 0.01$; $***$, $P < 0.001$ compared with control tissue.

Using nuclear DNA fragmentation as a sign of cell death in the lesions, only a few degenerating cells were found (Fig. 4). Most of them, showing nuclear condensation of apoptosis and DNA fragmentation, were identified by double staining as W3/13-positive T-lymphocytes. In addition, some CNP-positive oligodendrocytes showed nuclear condensation and fragmentation (Fig. 4). No such changes were observed in oligodendrocytes that expressed PLP mRNA.

Pattern 2

Sharply demarcated plaques, completely devoid of myelin sheaths, were the hallmark of pattern 2 of the demyelinating process (Fig. 5a). These lesions were in general surrounded by a broad zone of virus-infected tissue with similar structural alterations as those described for pattern 1 lesions (Fig. 5c). Like pattern 1 lesions, both the number of cells expressing PLP mRNA as well as the extent of mRNA expression in individual cells were reduced. Virus antigen expression within the demyelinated plaques was restricted to very few glial cells. The plaques were associated with a severe inflammatory reaction, the inflammatory infiltrates being mainly composed of lymphocytes and very high numbers of macrophages (Fig. 1). Lipid-laded macrophages strongly expressed the lysosomal marker ED1 and contained intracytoplasmic granules, reactive for all major and minor myelin proteins (MBP, PLP, MOG, and CNP; Fig. 5g,h). Glial fibrillary acidic protein (GFAP)-positive astrocytes were increased at the plaque borders but reduced in the center (Fig. 5i).

In the immediate vicinity of the demyelinated lesions, ongoing myelin and oligodendrocyte destruction was present, and dying glial cells with DNA fragmentation were mainly concentrated in these regions (Fig. 4). By immunochemistry (CNP, MOG) and in situ hybridization (PLP mRNA), most dying glial cells were oligodendrocytes. Most glial cells labeled by IST also expressed abundant virus protein. Morphologically, dying oligodendrocytes showed swollen cytoplasm and nuclei with rupture of nuclear membranes (Fig. 6a). This pattern is different from the nuclear condensation and fragmentation of apoptosis and was interpreted as necrotic cell death. However, dying cells labeled by anti-CNP or anti-MOG antibodies and showing nuclear alterations of apoptosis were present as well (Fig. 6c). In addition, many cells with the nuclear changes of apoptosis were identified by immunochemistry to be W3/13 positive T-lymphocytes (Fig. 6b; Barac-Latas et al., 1995).

Oligodendrocytes, reactive for myelin proteins or PLP mRNA, were lost in part of the lesions (Fig. 3). However, side by side with the demyelinating lesions, a variable degree of remyelination was present at this stage of the disease. Remyelinated areas were mainly located in the center of the demyelinated plaques and were dominated by high numbers of oligodendrocytes with an intensity of PLP mRNA expression that by far
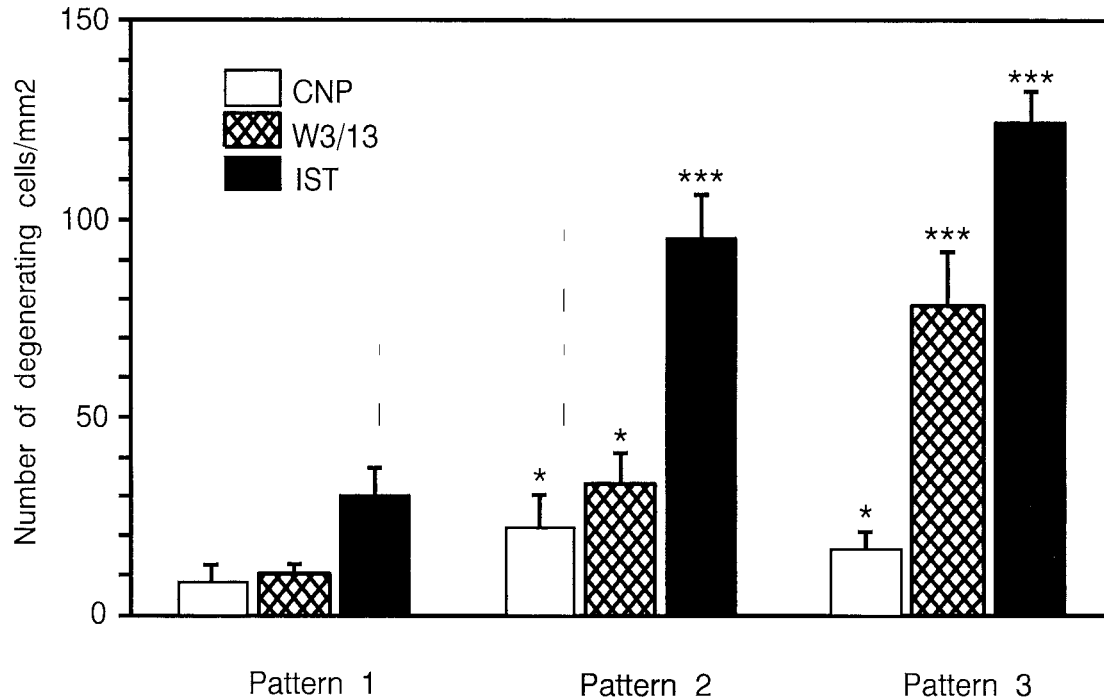
Fig. 4. The number of apoptotic oligodendrocytes and T-lympho-cytes, identified by nuclear morphology and double staining with anti-CNP and W3/13 as shown in Figure 6 in comparison with total numbers of dying cells visualized by in situ tailing. The following areas were evaluated: pattern 1, area of virus antigen expression; pattern 2, active demyelinating plaque plus surrounding area of virus antigen expression; pattern 3, actively demyelinating plaque. *, $P < 0.05$; **, $P < 0.01$; ***, $P < 0.001$ in comparison with pattern 1.

exceeded that in comparable white matter areas of uninfected controls or in unaffected "normal" white matter of the same animal (Figs. 3, 5b,e). In addition, a variable number of thin myelin sheaths were detected by immunochemistry with anti-MBP or anti-PLP anti-bodies. Only few oligodendrocytes in these remaining lesions expressed MOG. No virus antigen was present in astrocytes or oligodendrocytes in the remyelinating areas (Fig. 5f).

Pattern 3

The third type of lesions was characterized by intense inflammation and ongoing demyelination or tissue de-struction (Fig. 7a,c). However, virus antigen expression during this stage was minimal and was restricted to a very few glial cells in particular astrocytes in the demyelinated plaques or in the surrounding nervous system tissue (Fig. 7d,f). Within the lesions we found a pronounced reduction in immunoreactivity for MBP and PLP, and of cells expressing MOG, CNP or GFAP as well as PLP mRNA (Fig. 7b,e). This finding suggests that in addition to myelin, a significant number of oligodendrocytes and astrocytes was also destroyed in the plaques. However, axons were preserved, in part freely traversing the plaques between the infiltrating macrophages. The lesions were surrounded by dense GFAP-reactive astroglial scar tissue.

Ongoing demyelinating activity in these lesions was suggested by the presence of early myelin degradation

products in macrophages that still were immunoreac-tive for all myelin proteins, including MBP, PLP, MOG, and CNP. Numerous cells within the lesions showed DNA fragmentation. Cells with DNA fragmentation together with nuclear condensation and fragmentation, typical of apoptosis, were partly identified by immuno-cytochemistry as T-lymphocytes. In addition, dying cells, labeled either by in situ hybridization for PLP mRNA or by immunocytochemistry for MOG and CNP were found in particular at the edge of the plaques (Figs. 4, 6d). No virus antigen or RNA expression was found in dying cells in this type of lesions.

At late stages after virus infection (three rats sampled later than 60 days), residual lesions were present in the brain and spinal cord. No inflammation and no virus antigen expression was found. In the brain, some atrophy of the gray and white matter, together with dilatation of cerebral ventricles, was noted. In addition, focal areas with extensive astrocytic gliosis and some

Fig. 5. Morphological changes in pattern 2. Serial sections were stained with luxol fast blue (a,d,g); in situ hybridization for PLP mRNA (b,e); virus antigen (c,f), ED1-positive macrophages (h) and GFAP (i). The asterisks label identical landmarks in the respective low and high magnification pictures. The center of the demyelinating lesion (a,d) contains a high density of cells with PLP mRNA expression (b,e) and apparently represents an area of remylination. This area is free of virus antigen. This center is surrounded by a zone with complete lack of PLP mRNA reactive cells, which in part is demyelin-ated or—at the margin—is actively, demyelinating, as shown by the presence of macrophages with myelin degradation products (g). Virus antigen is predominantly present at the zone of active demyelination (c,f) and in the adjacent white matter. a–c, ×20; d–f,h,i, ×160; g, ×250.
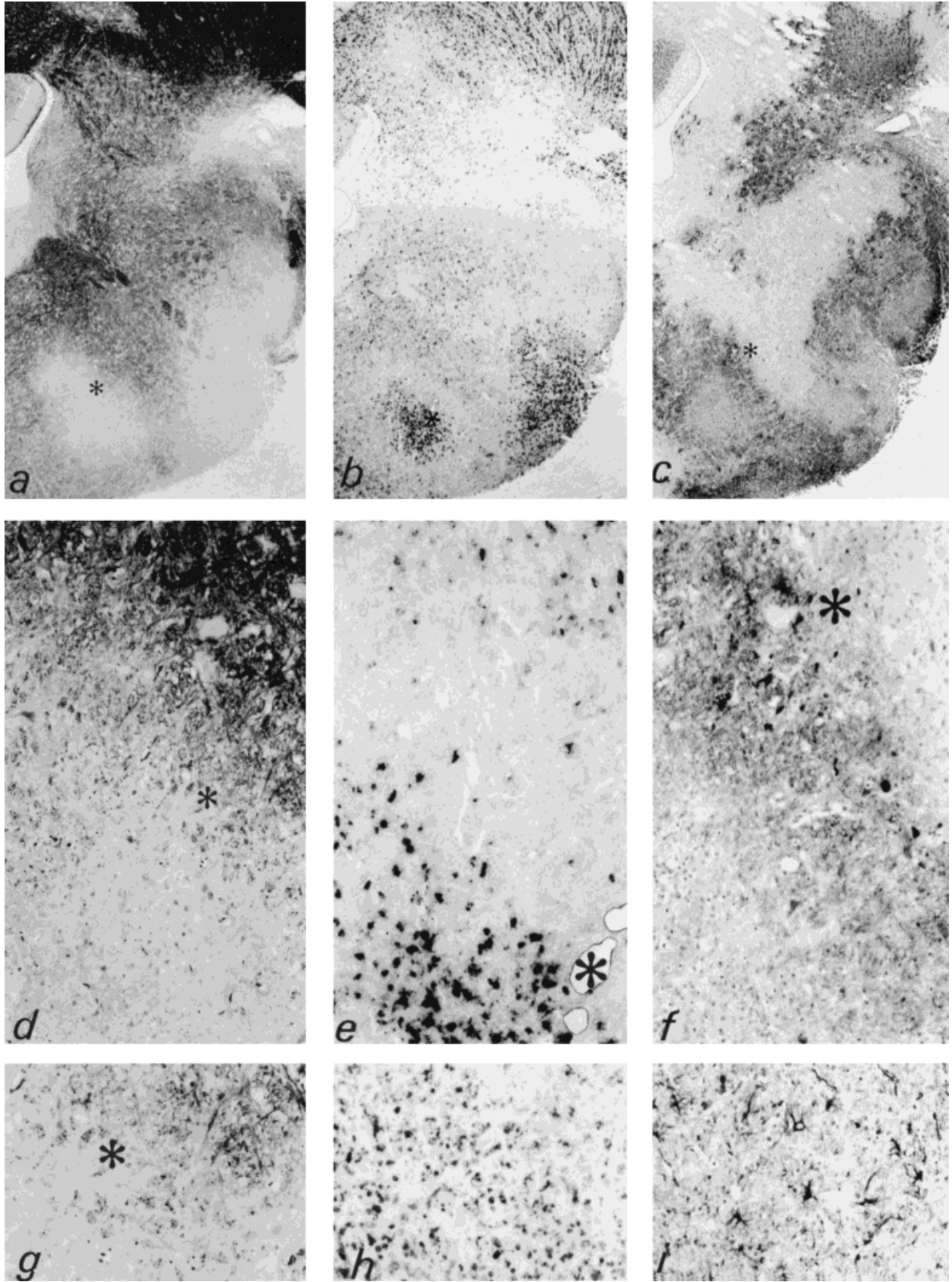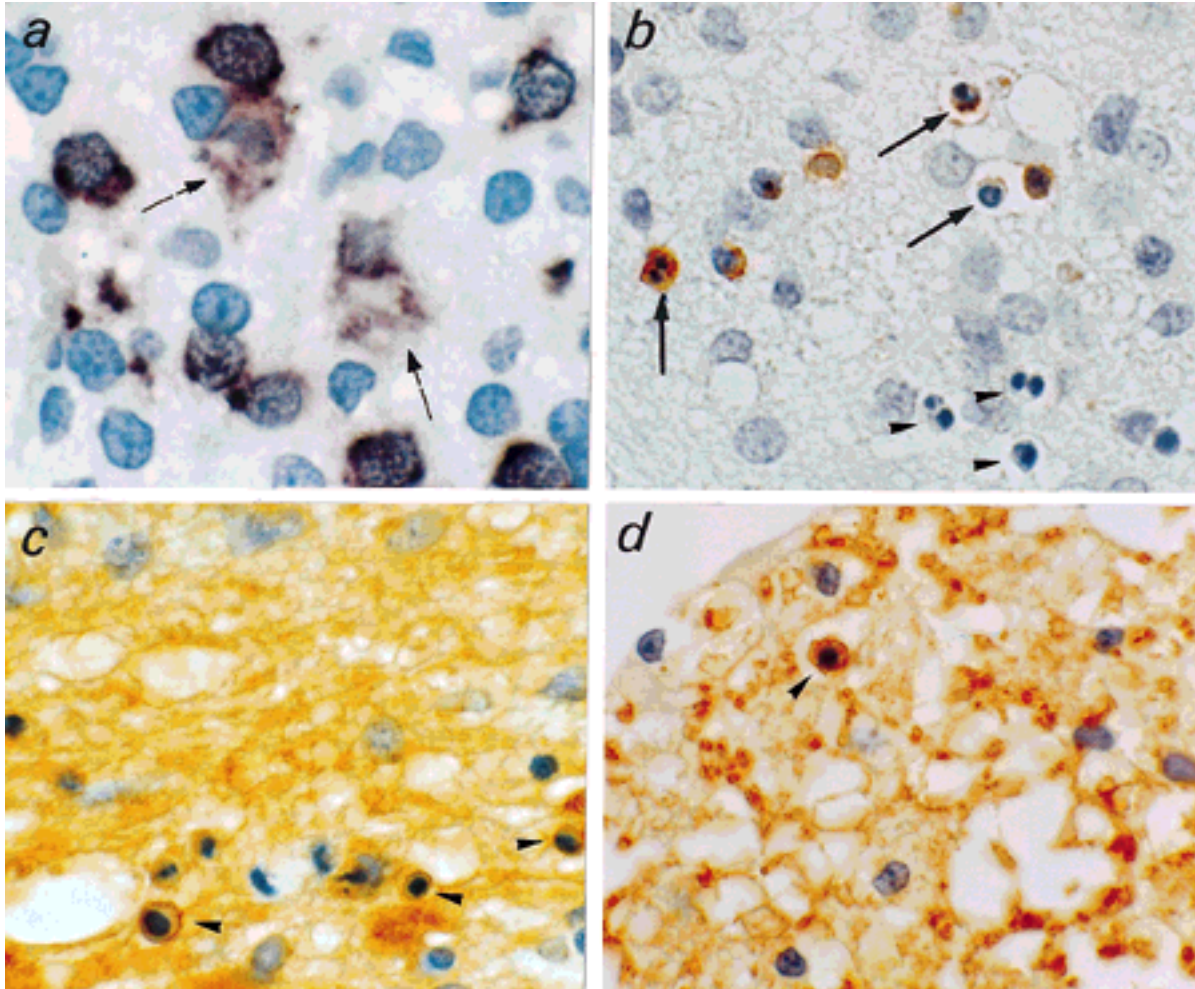
Fig. 5.

Fig. 6. Patterns of cell destruction. **a:** Oligodendrocytes from pattern 2 lesions, stained with in situ hybridization for PLP mRNA; two cells (arrows) with cytoplasmic and nuclear swelling and cell fragmentation suggest necrosis; ×1,000. **b:** Pattern 2 lesions stained with W3/13. Several immunostained T-cells (arrows) and W3/13-negative cells (arrowheads) with nuclear condensation and fragmentation suggest apoptosis; ×1,000. **c:** Edge of a pattern 2 lesion, stained with anti-CNP. Oligodendrocytes with nuclear condensation suggest of apoptosis (arrowheads); ×800. **d:** Pattern 3 lesion stained with anti-CNP; oligodendrocyte with nuclear condensation; ×800.

reduction of axonal density were found, which, however, revealed a normal density of myelin sheaths. These areas apparently represent remyelinated lesions.

In contrast, in the spinal cord large lesions persisted. They were surrounded by a dense astrocytic scar. In the center of the lesions GFAP as well as PLP protein and PLP mRNA positive cells were absent. Nerve fibers within the plaques were remyelinated by Schwann cells.

Time Dependent Development and Size of the Lesions at Different Stages of the Disease

Lesions with structural abnormalities following patterns 1 and 2 were found significantly earlier after infection than those with pattern 3. This suggests that the above-described lesional patterns indeed reflect stages of lesion formation (Table 1).

Whereas during early stages of the disease glial cells were infected by coronavirus in large areas of the brain and spinal cord, the actual demyelinated areas in patterns 2 and 3 were much smaller and focal, with very little virus antigen expression. These data suggest that virus infection taking place during the first stage of SDE may be cleared in part by a mechanism that does not lead to destruction of infected glial cells or demyelination.

DISCUSSION

Virus-induced chronic demyelination of the CNS has raised considerable attention as a possible model of disease for multiple sclerosis (Dal Canto and Rabinowitz, 1981; Kyuwa and Stohlman, 1990). Chronic demyelinated plaques in the CNS in experimental animals can be induced by a variety of virus infections, including Theiler's virus, coronavirus MHV-JHM, canine
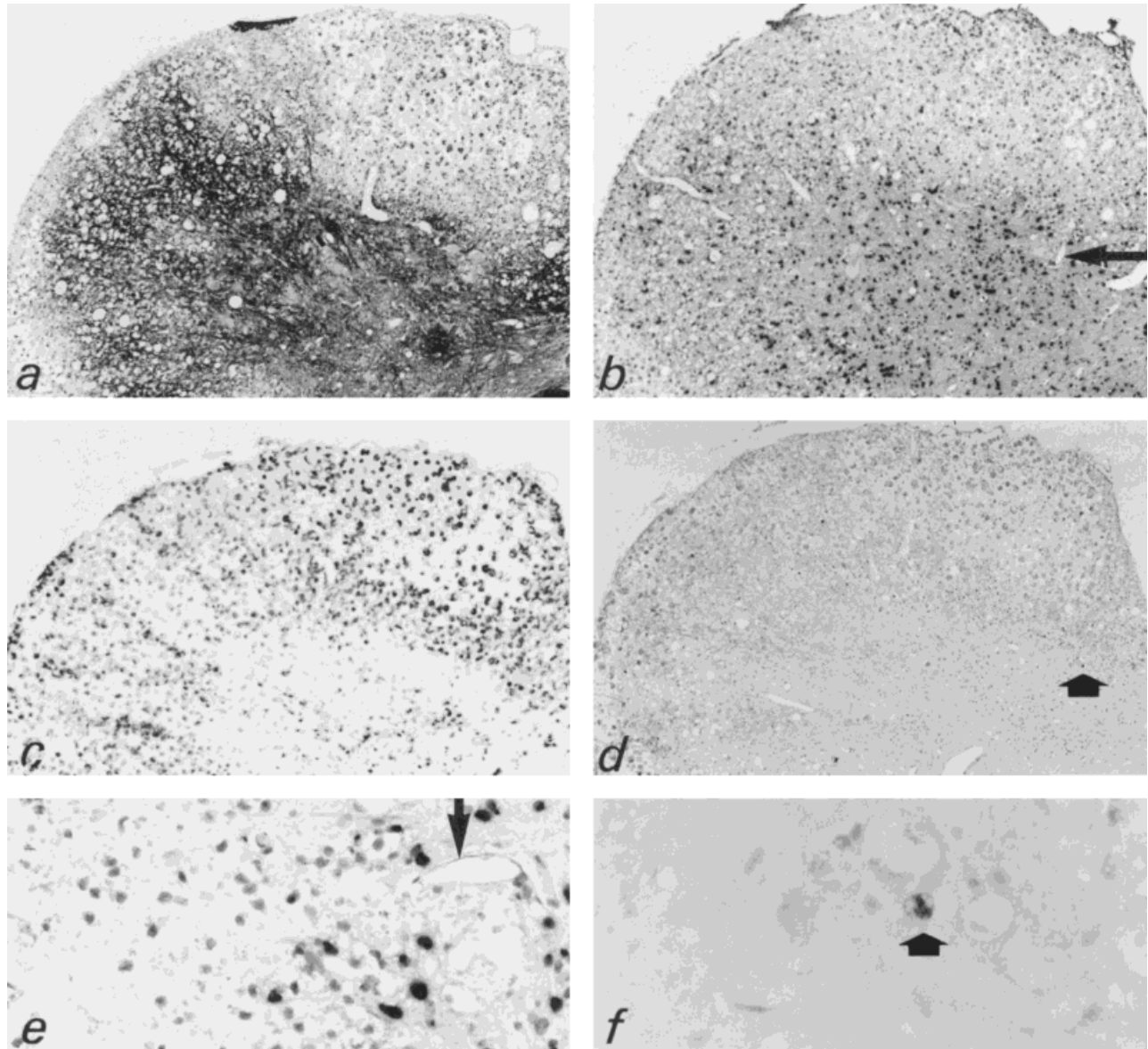
Fig. 7. Morphological changes of pattern 3. Serial sections stained with luxol fast blue (a), in situ hybridization for PLP mRNA with nuclear counterstain (b,e); ED1-positive macrophages (c) and virus antigen (d,f). The lesions are large demyelinated plaques with rarefaction of the tissue texture **(a)** and pronounced macrophage infiltration **(c).** PLP mRNA containing cells (dark black cells in **b** and **e**) are lost in the lesions. There is very little virus antigen expression **(d,f).** The arrows in b and e or d and f label identical structures in low and high magnification. a–d, ×85; e, ×340; f, ×800.

distemper virus, Semliki Forest virus, herpes simplex virus, visna virus, and others (Brankin, 1996; Dal Canto and Rabinowitz, 1981).

All these diseases are characterized by persistent virus infection, chronic inflammation, and the formation of confluent demyelinated lesions. However, in spite of extensive research in these models the mechanisms finally leading to the destruction of myelin sheaths in vivo are controversial. Possible mechanisms of demyelination, suggested in a variety of in vitro and in vivo studies, include direct cytolytic infection of oligodendrocytes (Rosenthal et al., 1986), specific T-cell-mediated cytotoxicity directed against infected oligodendrocytes (Lindsley et al., 1991; Subak-Sharpe et al.,

1993), "by-stander demyelination" induced by toxic products of activated macrophages (Botteron et al., 1992; Griot et al., 1989), and antibody-mediated immune reactions, directed against autoantigens or virus proteins that are expressed on the surface of infected oligodendrocytes (Fujinami et al., 1989; Zimprich et al., 1991). Finally, metabolic disturbances of oligodendrocytes, induced by their infection, could lead to instability of the myelin/oligodendrocyte complex and demyelination (Jordan et al., 1989; Rodriguez et al., 1994).

To test the relevance of these different mechanisms for the natural course of coronavirus encephalomyelitis, a detailed analysis of the patterns of demyelination and the fate of oligodendrocytes in the lesions is re-

quired. In the present study we have tried to achieve this by using new tools to identify oligodendrocytes and their cytopathic reaction, which recently became available and have also been used for similar studies in multiple sclerosis lesions (Brueck et al., 1994; Ozawa et al., 1994). Our data suggest that the mechanisms of oligodendrocyte damage may be complex in vivo and may partly depend on the stage of the demyelinating process.

During the first stage we observed a massive downregulation of PLP mRNA in infected oligodendrocytes, a pattern similar to that described in coronavirus encephalomyelitis in mice (Jordan et al., 1989) and in Theiler's virus-induced demyelinating encephalomyelitis (Ozden et al., 1993; Rodriguez et al., 1994; Yamada et al., 1990). This finding suggests that virus infection of oligodendrocytes, although not directly cytolytic, may block their "luxury function" of maintaining the supply of myelin proteins. However, this mechanism alone is apparently insufficient to induce demyelinated plaques since the same virus infection in immunodeficient nude mice does not lead to the destruction of myelin. Furthermore, virus infection at this stage of the disease was much more widespread than demyelination at later stages, suggesting that virus can be cleared from infected glial cells, without leading to their direct or immune-mediated lysis. Such a mechanism could be mediated by direct anti-viral effects of certain cytokines such as gamma-interferon (Pearce et al., 1994; Stohlman et al., 1995).

During the second stage demyelinated plaques were formed. As has been shown before, myelin destruction was associated with a variable loss of PLP mRNA expressing oligodendrocytes in the lesions. At the margin of the lesions we observed ongoing destruction of virus-infected oligodendrocytes by the pattern of cell necrosis. Whereas direct T-cell-mediated cytotoxicity or destruction of oligodendrocytes by macrophage toxins such as tumor necrosis factor (Selmaj et al., 1991) or oxygen radicals (Griot et al., 1989) appear to be mediated by apoptosis, necrosis is the dominant pattern of cell death in antibody- and complement-mediated cytotoxicity. We have shown previously that in coronavirus-induced SDE virus-envelope proteins are expressed on the extracellular surface of oligodendrocytes and immunoglobulin and complement C9 are deposited in actively demyelinating lesions (Zimprich et al., 1991). Furthermore, in SDE animals neutralizing antibodies against viral S-proteins are mainly present in the chronic stage, when demyelination takes place (Flory et al., 1995; Koga et al., 1984; Schwender et al., 1991). Thus, our present results identifying necrosis of infected oligodendrocytes further indicate that demyelination in this second stage of the disease may be mediated by neutralizing anti-viral antibodies, which have access to the brain tissue in the course of the T-cell-mediated inflammatory reaction and recognize their antigen on the surface of infected oligodendrocytes. Final destruction of myelin sheaths may then be accomplished by complement or by macrophages, which

become activated by the T-cell-mediated immune reaction. A similar mechanism has been found to operate in the majority of models of demyelinating chronic autoimmune encephalomyelitis, albeit directed in that case not against virus, but autoantigens (Linington and Lassmann 1987; Linington et al., 1988; Piddelsden et al., 1991, 1993).

Most of the above-described lesions showed some degree of remyelination in the center of the demyelinated plaques. It is not clear whether the remyelinating oligodendrocytes are derived from cells that have escaped destruction during active demyelination or whether they were recruited from progenitor cells. However, several observations suggest that the latter interpretation is accurate. In the areas of active demyelination extensive destruction of oligodendrocytes took place, and no oligodendrocytes could be detected in demyelinating areas by any of the different markers that have been used in the present study. Furthermore, the oligodendrocytes in the remyelinating lesions massively expressed PLP mRNA but were not stained by anti-MOG antibodies. MOG is a protein that is expressed late in myelination and is absent on early progenitor cells (Matthieu and Amiguet, 1990). It is, however, preserved on oligodendrocytes that have survived the demyelinating process, as shown in Wallerian degeneration (Ludwin, 1990). Thus, the absence of MOG reactivity on remyelinating cells indicates that these cells may come from the progenitor cell pool and have not yet reached the final stage of differentiation into mature oligodendrocytes (Ozawa et al., 1994).

The patterns of myelin and oligodendrocyte pathology were fundamentally different in the third stage of this disease. In this stage virus antigen as well as virus RNA was detectable only in a small minority of glial cells, in particular in astrocytes. However, progressive destruction of myelin sheaths and oligodendrocytes took place, reflected by the presence of macrophages containing early products of myelin degradation and abundant oligodendrocytes with nuclear DNA fragmentation. Oligodendrocyte death was structurally accompanied by condensation and fragmentation of their nuclei, suggesting apoptosis as the main destructive mechanism. Neither by immunocytochemistry nor by in situ hybridization were we able to detect coronavirus protein or mRNA in the dying oligodendrocytes. Actively demyelinating lesions were massively infiltrated by macrophages together with some T-lymphocytes. These data suggest that in late stages of the demyelinating process, when virus infection is cleared from most cells in the lesions, immune-mediated demyelination and oligodendrocyte destruction may still continue. It is tempting to speculate that at this stage of the disease demyelination is mainly accomplished by a bystander mechanism (Wisniewski and Bloom, 1975), mediated by toxic products that are produced by activated macrophages in the lesions (Stoner et al., 1977). Possible candidates for macrophage toxins, which may induce apoptosis in target cells, are tumor necrosis factor (Selmaj and Raine, 1988; Selmaj et al., 1991) or reactive

oxygen species (Griot et al., 1989). Alternatively, a low degree of oligodendroglia infection, which is not detectable by our methods of immunocytochemistry or in situ hybridization, may be recognized by cytotoxic T-cells and may lead to programmed cell death of oligodendrocytes. Finally, cytotoxic T-cell reactions, for instance against stress proteins in oligodendrocytes (Freedman et al., 1991), may be involved in the induction of oligodendrocyte apoptosis. Although no data are available in the model of coronavirus-induced SDE, both an increased infiltration of the CNS tissue by gamma/delta T-lymphocytes and upregulation of stress proteins in oligodendrocytes have been described to appear in chronic inflammatory brain lesions of autoimmune encephalomyelitis (Gao et al., 1995).

In conclusion, our data provide further evidence that the mechanisms of demyelination in a model of virus-induced inflammatory demyelinating disease are complex and may be mediated through a combination of metabolic changes, by immune-mediated destruction of infected oligodendrocytes, and by "bystander damage" of uninfected cells. Although these different mechanisms may operate side by side in the same animal, there is an apparent dominance of the individual patterns at defined stages of the disease process. Interestingly, a similar variability in the patterns of demyelination and oligodendrocyte death has recently been observed to occur in the lesions of different MS patients and at different stages of disease evolution of MS (Brueck et al., 1994; Ozawa et al., 1994). It can be expected that a detailed comparison of the patterns of demyelination between different experimental models of virus-induced or autoimmune-mediated demyelination and human disease will resolve some of the controversial issues of the pathogenesis of demyelination in multiple sclerosis.

REFERENCES

Barac-Latas, V., Wege, H., and Lassmann, H. (1995) Apoptosis of T lymphocytes in coronavirus-induced encephalomyelitis. *Reg. Immunol.,* 6:355–357.

Brankin, B. (1996) Viruses in multiple sclerosis models. *Int. MSJ.,* 2:51–59.

Botteron, C., Zurbriggen, A., Griot, C., and Vandevelde, M. (1992) Canine distemper virus-immune complexes induce bystander degeneration of oligodendrocytes. *Acta Neuropathol. (Berl.),* 83:402–407.

Breitschopf, H., Suchanek, G., Gould, R.M., Colman, D.R., and Lassmann, H. (1992) *In situ* hybridization with digoxigenin-labeled probes: Sensitive and reliable detection method applied to myelinating rat brain. *Acta Neuropathol.,* 84:581–587.

Bruek, W., Schmied, M., Suchanek, G., Brueck, Y., Breitschopf, H., Poser, S., Piddlesden, S., and Lassmann, H. (1994) Oligodendrocytes in the early course of multiple sclerosis. *Ann. Neurol.,* 35:65–73.

Colman, D.R., Kreibich, G., Frey, A.B., and Sabatini, D.D. (1982) Synthesis and incorporation of myelin polypeptides into CNS myelin. *J. Cell Biol.,* 95:598–608.

Dal Canto, M.C. and Rabinowitz, S.G. (1981) Experimental models of virus-induced demyelination of the central nervous system. *Ann. Neurol.,* 11:109–127.

Fleming, J.O., Wang, F.I., Trousdale, M.D., Hinton, D.R., and Stohlman, S.A. (1993) Interaction of immune and central nervous systems: Contribution of anti-viral Thy-1+ cells to demyelination induced by coronavirus JHM. *Reg. Immunol.,* 5:37–43.

Flory, E., Stuehler, A., Barac-Latas, V., Lassmann, H., and Wege, H. (1995) Coronavirus-induced encephalomyelitis: Balance between protection and immune pathology depends on the immunization schedule with spike protein S. *J. Gen. Virol.,* 76:873–879.

Freedman, M., Ruijs, T., Selin, L., and Antel, J. (1991) Peripheral blood gamma-delta T cells lyse fresh human brain-derived oligodendrocytes. *Ann. Neurol.,* 30:794–800.

Fujinami, R.S., Rosenthal, A., Lampert, P.W., Zurbriggen, A., and Yamada, M. (1989) Survival of athymic (nu/nu) mice after Theiler's murine encephalomyelitis virus infection by passive administration of neutralizing monoclonal antibody. *J. Virol.,* 63:2081–2087.

Gao, Y.L., Brosnan, C.F., and Raine, C.S. (1995) Experimental autoimmune encephalomyelitis. Qualitative and semiquantitative differences in heat shock protein 60 expression in the central nervous system. *J. Immunol.,* 154:3548–3556.

Gold, R., Schmied, M., Giegerich, G., Breitschopf, H., Hartung, H.P., Toyka, K.V., and Lassmann, H. (1994) Differentiation between cellular apoptosis and necrosis by combined use of *in situ* tailing and nick translation techniques. *Lab Invest.,* 71:219–225.

Griot, C., Burge, T., Vandevelde, M., and Peterhans, E. (1989) Antibody-induced generation of reactive oxygen radicals by brain macrophages in canine distemper encephalitis: A mechanism for bystander demyelination. *Acta Neuropathol., (Berl.),* 78:396–403.

Gunn, C.A., Richards, M.K., and Linington, C. (1990) The immune response to myelin proteolipid protein in the Lewis rat: Identification of the immunodominant B cell epitope. *J. Neuroimmunol.,* 27:155–162.

Iseki, S. (1986) DNA strand breaks in rat tissues as detected by *in situ* nick translation. *Exp. Cell Res.,* 167:311–326.

Jordan, C.A., Friedrich, V.L. Jr., Godfraind, C., Cardellechio, C.B., Holmes, K.V., and Dubois-Dalcq, M. (1989) Expression of viral and myelin gene transcripts in a murine CNS demyelinating disease cause by a coronavirus. *Glia,* 2:318–329.

Koga, M., Wege, H., and ter Meulen, V. (1984) Sequence of murine coronavirus JHM induced neruophatological changes in rats. *Neuropathol. Appl. Neurobiol.,* 10:173–184.

Koerner, H., Schliephake, A., Winter, J., Zimprich, F., Lassmann, H., Sedgwick, J., Siddell, S., and Wege, H. (1991) Nucleocapsid or spike protein-specific CD4⁻ T lymphocytes protect against coronavirus-induced encephalomyelitis in the absence of CD8⁻ T cells. *J. Immunol.,* 147:2317–2323.

Kyuwa, S. and Stohlmann, S.A. (1990) Pathogenesis of a neurotropic murine coronavirus, strain JHM in the central nervous system of mice. *Semin. Virol.,* 1:273–280.

Lindsley, M.D., Thiemann, R., and Rodriguez, M. (1991) Cytotoxic T cells isolated from the central nervous system of mice infected with Theiler's virus. *J. Virol.,* 65:6612–6620.

Linington, C., and Lassmann, H. (1987) Antibody responses in chronic relapsing experimental allergic encephalomyelitis: Correlation of serum demyelinating activity with antibody titre to the myelin/oligodendroglia glycoprotein (MOG). *J. Neuroimmunol.,* 17:61–69.

Linington, C., Bradl, M., Lassmann, H., Brunner, C., and Vass, K. (1988) Augmentation of demyelination in rat acute allergic encephalomyelitis by circulating mouse monoclonal antibodies against myelin/oligodendroglia glycoprotein. *Am. J. Pathol.,* 130:443–454.

Ludwin, S.K. (1990) Oligodendrocyte survival in Wallerian degeneration. *Acta Neuropathol. (Berl.),* 80:184–191.

Matthieu, J.-M. and Amiguet, P. (1990) Myelin/oligodendrocyte glycoprotein expression during development in normal and myelin-deficient mice. *Dev. Neurosci.,* 12:293–302.

Nagashima, K., Wege, H., Meyermann, R., and ter Meulen, V. (1978) Corona virus induced subacute demyelinating encephalomyelitis in rats: A morphological analysis. *Acta Neuropathol. (Berl.),* 44:63–70.

Nagashima, K., Wege, H., Meyermann, R., and ter Meulen, V. (1979) Demyelinating encephalomyelitis induced by longterm corona virus infection in rats. *Acta Neuropathol. (Berl.),* 45:205–213.

Ozawa, K., Suchanek, G., Breitschopf, H., Brueck, W., Budka, H., Jellinger, K., and Lassmann, H. (1994) Patterns of oligodendroglia pathology in multiple sclerosis. *Brain,* 117:1311–1322.

Ozden, S., Aubert, C., Bureau, J.F., Gonzales-Dunia, D., and Brahic, M. (1993) Analysis of proteolipid protein and PO transcripts in mice infected with Theiler's virus. *Microbiol. Pathol.,* 14:123–131.

Pearce, B.D., Hobbs, V., McGraw, T.S., and Buchmeier, M.J. (1994) Cytokine induction during T-cell-mediated clearance of mouse hepatitis virus from neurons in vivo. *J. Virol.,* 68:5483–5495.

Piddlesden, S., Lassmann, H., Laffafian, I., Morgan, B.P., and Linington, C. (1991) Antibody-mediated demyelination in experimental allergic encephalomyelitis is independent of complement membrane attack complex formation. *Clin. Exp. Immunol.,* 83:245–250.

Piddlesden, S., Lassmann, H., Zimprich, F., Morgan, B.P., and Linington, C. (1993) The demyelinating potential of antibodies to myelin oligodendrocyte glycoprotein is related to their ability to fix complement. *Am. J. Pathol.,* 143:555–564.

Rodriguez, M., Prayoonwiwat, N., Howe, C., and Sanborn, K. (1994) Proteolipid protein gene expression in demyelination and remyelination of the central nervous system: A model for multiple sclerosis. *J. Neuropathol. Exp. Neurol.,* 53:136–143.

Rosenthal, A., Fujinami, R.S., and Lampert, P.W. (1986) Mechanisms of Theiler's virus-induced demyelination in nude mice. *Lab. Invest.,* 54:515–522.

Schwender, S., Imrich, H., and Doerries, R. (1991) The pathogenic role of virus specific antibody-secreting cells in the central nervous system of rats with different susceptibility to coronavirus-induced demyelinating encephalitis. *Immunology,* 74:533–538.

Selmaj, K.W. and Raine, C.S. (1988) Tumor necrosis factor mediates myelin and oligodendrocyte damage in vitro. *Ann. Neurol.,* 23:339–346.

Selmaj, K., Raine, C.S., Farooq, M., Norton, W.T., and Brosnan, C.F. (1991) Cytokine cytotoxicity against oligodendrocytes. Apoptosis induced by lymphotoxin. *J. Immunol.,* 147:1522–1529.

Sorensen, O., Perry, D., and Dales, S. (1980) In vivo and in vitro models of demyelinating diseases. III. JHM virus infection of rats. *Arch. Neurol.,* 37:478–484.

Stohlman, S.A., Bergmann, C.C., van der Veen, R.C., and Hinton, D.R. (1995) Mouse hepatitis virus-specific cytotoxic T lymphocytes protect from lethal infection without eliminating virus from the central nervous system. *J. Virol.,* 69:684–694.

Stoner, G.L., Brosnan, C.F., Wisniewski, H.M., and Bloom, B.R. (1977) Studies on demyelination by activated lymphocytes in the rabbit eye. I. Effects of a mononuclear cell infiltrate influenced by products of activated lymphocytes. *J. Immunol.,* 118:2094–2102.

Subak-Sharpe, I., Dyson, H., and Fazakerly, J. (1993) In vivo depletion of CD8⁻ T cells prevents lesions of demyelination in Semliki Forest virus infection. *J. Virol.,* 67:7629–7633.

Vass, K., Lassmann, H., Wekerle, H., and Wisniewski, H.M. (1986) The distribution of Ia-antigen in the lesions of rat acute experimental allergic encephalomyelitis. *Acta Neuropathol. (Berl.),* 70:149–160.

Vass, K., Berger, M.L., Nowak, T.S., Welch, W.J., and Lassmann, H. (1989) Induction of stress protein HSP70 in nerve cells after status epilepticus in the rat. *Neurosci. Lett.,* 100:259–264.

Wang, F.I., Stohlman, S.A., and Fleming, J.O. (1990) Demyelination induced by murine hepatitis virus JHM strain (MHV-4) is immunologically mediated. *J. Neuroimmunol.,* 30:31–41.

Wege, H., Watanabe, R., and ter Meulen, V. (1984) Relapsing subacute demyelinating encephalomyelitis in rats in the course of coronavirus JHM infection. *J. Neuroimmunol.,* 6:325–336.

Wege, H., Schliephake, A., Koerner, H., Flory, E., and Wege, H. (1993) An immunodominant CD4⁻ T cell site on the nucleocapsid protein of murine coronavirus contributes to protection against encephalomyelitis. *J. Gen. Virol.,* 74:1287–1294.

Winter, J. (1992) Coronavirus-Persistenz in Hirnzellen-Untersuchungen zur Pathogenese von Entmarkungsenzephalomyelitiden. Doctoral thesis, University of Wuerzburg.

Wisniewski, H.M. and Bloom, B.R. (1975) Primary demyelination as a nonspecific consequence of a cell mediated immune reaction. *J. Exp. Med.,* 141:346–359.

Yamada, M., Zurbriggen, A., and Fujinami, R.S. (1990) The relationship between viral RNA, myelin-specific mRNA's, and demyelination in central nervous system disease during Theiler's virus infection. *Am. J. Pathol.,* 137:1467–1479.

Zimprich, F., Winter, H., Wege, H., and Lassmann, H. (1991) Coronavirus induced primary demyelination: Indications for the involvement of a humoral immune response. *Neuropathol. Appl. Neurobiol.,* 17:469–484.